RSC Advances

PAPER

View Article Online
View Journal | View Issue

Cite this: *RSC Adv.*, 2019, **9**, 10201

Mechanistic insight into the catalytic hydrogenation of nonactivated aldehydes with a Hantzsch ester in the presence of a series of organoboranes: NMR and DFT studies†

Go Hamasaka, [ab] Hiroaki Tsuji, [ab] Masahiro Ehara [ab] and Yasuhiro Uozumi *[abc]

Mechanistic studies on the organoborane-catalyzed transfer hydrogenation of nonactivated aldehydes with a Hantzsch ester (diethyl-2,6-dimethyl-1,4-dihydropyridine-3,5-dicarboxylate) as a synthetic NADH analogue were performed by NMR experiments and DFT calculations. In the reaction of benzaldehyde with the Hantzsch ester, the catalytic activity of tris[3,5-bis(trifluoromethyl)phenyl]borane was superior to that of other borane catalysts, such as tris(pentafluorophenyl)borane, trifluoroborane etherate, or triphenylborane. Stoichiometric NMR experiments demonstrated that the hydrogenation process proceeds through activation of the aldehyde by the borane catalyst, followed by hydride transfer from the Hantzsch ester to the resulting activated aldehyde. DFT calculations for the hydrogenation of benzaldehyde with the Hantzsch ester in the presence of borane catalysts supported the reaction pathway and showed why the catalytic activity of tris[3,5-bis(trifluoromethyl)phenyl]borane is higher than that of the other boron catalysts. Association constants and Gibbs free energies in the reaction of boron catalysts with benzaldehyde or benzyl alcohol, which were investigated by ^{1}H NMR analyses, also indicated why tris[3,5-bis(trifluoromethyl)phenyl]borane is a superior catalyst to tris(pentafluorophenyl) borane, trifluoroborane etherate, or triphenylborane in the hydrogenation reaction.

Received 26th February 2019
Accepted 25th March 2019

DOI: 10.1039/c9ra01468c

rsc.li/rsc-advances

Introduction

Biological hydrogenation processes are recognized as important reactions in nature. These processes are mediated by a combination of an enzyme and an organic reduction cofactor (*e.g.*, NADH or NADPH).[1] In particular, the biological hydrogenation of acetaldehyde is a crucial final step in the fermentation of sugars to form ethanol. The reaction proceeds in the presence of alcohol dehydrogenase and NADH under anaerobic conditions. The reaction pathway of this process is known to be as follows: (1) acetaldehyde is activated by coordination of its carbonyl group to the Zn center of alcohol dehydrogenase; and (2) hydride is transferred to the activated acetaldehyde from NADH (Fig. 1).[1,2]

In attempts to realize a biomimetic hydrogenation process, many organic chemists have investigated the catalytic hydrogenation of imines, α,β-unsaturated carbonyl compounds, or α-keto esters with a synthetic NADH analogue.[3–7] Despite numerous investigations of Brønsted or Lewis acid-catalyzed hydrogenations of nonactivated aldehydes with synthetic NADH analogues, no efficient hydrogenation system was developed until 2015.[8,9] In 2015, we reported the first example of an organoborane-catalyzed hydrogenation of nonactivated aliphatic and aromatic aldehydes with a Hantzsch ester (diethyl-2,6-dimethyl-1,4-dihydropyridine-3,5-dicarboxylate) as a synthetic NADH analogue to give the corresponding primary alcohols (Scheme 1).[10] In this reaction, tris[3,5-bis(trifluoromethyl)phenyl]borane showed superior catalytic

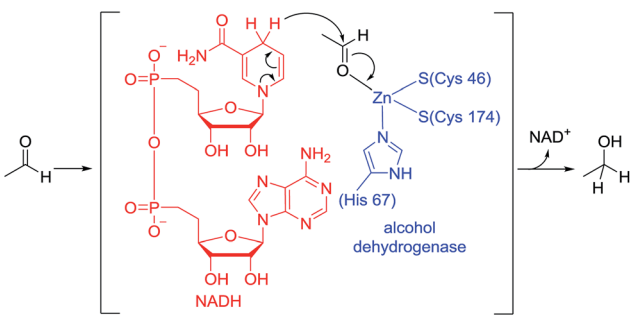

Fig. 1 Active site of alcohol dehydrogenase for the reduction of acetaldehyde with NADH.

[a]*Institute for Molecular Science (IMS), Myodaiji, Okazaki 444-8787, Japan. E-mail: uo@ims.ac.jp*

[b]*SOKENDAI (The Graduate University for Advanced Studies), Myodaiji, Okazaki 444-8787, Japan*

[c]*JST-ACCEL, Myodaiji, Okazaki 444-8787, Japan*

† Electronic supplementary information (ESI) available: Experimental and computational details. See DOI: 10.1039/c9ra01468c

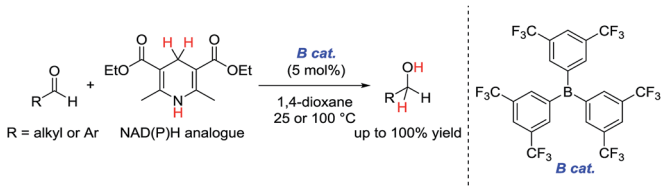

Scheme 1 Organoborane-catalyzed hydrogenation of nonactivated aldehydes with a Hantzsch ester (our previous work).

activity to other borane catalysts. However, the details of the reaction mechanism and the origin of the superiority of tris[3,5-bis(trifluoromethyl)phenyl]borane to the other borane catalysts were not clarified.

Because of their high oxophilic Lewis acidities, organoborane compounds such as tris(pentafluorophenyl)borane have been used as Lewis acid catalysts in various organic transformations including the Mukaiyama-aldol reaction and the Hosomi–Sakurai reaction.[11,12] These reactions proceed through coordination of the carbonyl compound to the boron catalyst (as exemplified by the formation of intermediate **Int-I** in Fig. 2a) followed by attack by a nucleophile (silyl enol ether or allyl silane) on the resulting activated carbonyl compound.

Electron-deficient borane compounds have also been used as partners in frustrated Lewis pair catalysts to promote the hydrogenation of unsaturated bonds with H_2.[13–15] In 2010, Stephan, Crudden, and co-workers discovered that borohydride species such as **Int-IV** in Fig. 2b are generated by the reaction of tris(pentafluorophenyl)borane with Hantzsch esters.[16] However, catalytic applications of these borohydrides were not investigated. Recently, Oestreich and co-workers reported that tris(pentafluorophenyl)borane catalyzes the hydrogenation of imines or related N-heterocycles with cyclohexa-1,4-dienes.[17,18] In this reaction, tris(pentafluorophenyl)borane abstracts hydrogen from the cyclohexa-1,4-diene to generate a borohydride species; this reaction is similar to that reported by Stephan and Crudden and co-workers.[16] This process is followed by reaction with the imine or a related N-heterocycle to give the corresponding hydrogenated product.

On the basis of the reaction pathways reported in the literature,[11–18] we propose two plausible reaction pathways for our organoborane-catalyzed hydrogenation of aldehydes with a Hantzsch ester, as shown in Fig. 2. The first of these proposed reaction pathways is shown in Fig. 2a. In this pathway, an aldehyde **1** is activated by a boron catalyst. Hydrogen is transferred to the activated aldehyde from the Hantzsch ester **2** to form an alcohol–boron adduct **Int-III** and the Hantzsch pyridine **4**. **Int-III** then dissociates to give an alcohol **3**, with the regeneration of the boron catalyst. The second possible reaction pathway is shown in Fig. 2b. This proceeds through generation of a borohydride species **Int-IV** by the reaction of **2** with the boron catalyst. **Int-IV** then reacts with **1** to give **Int-III**. Dissociation of **Int-III** to afford **3** is accompanied by regeneration of the boron catalyst.

Here, we report an investigation of the mechanism of our organoborane-catalyzed hydrogenation of aldehydes with a Hantzsch ester by means of NMR experiments and DFT calculations. We also discuss why tris[3,5-bis(trifluoromethyl)phenyl]borane shows a superior catalytic activity to that of other boron catalysts.

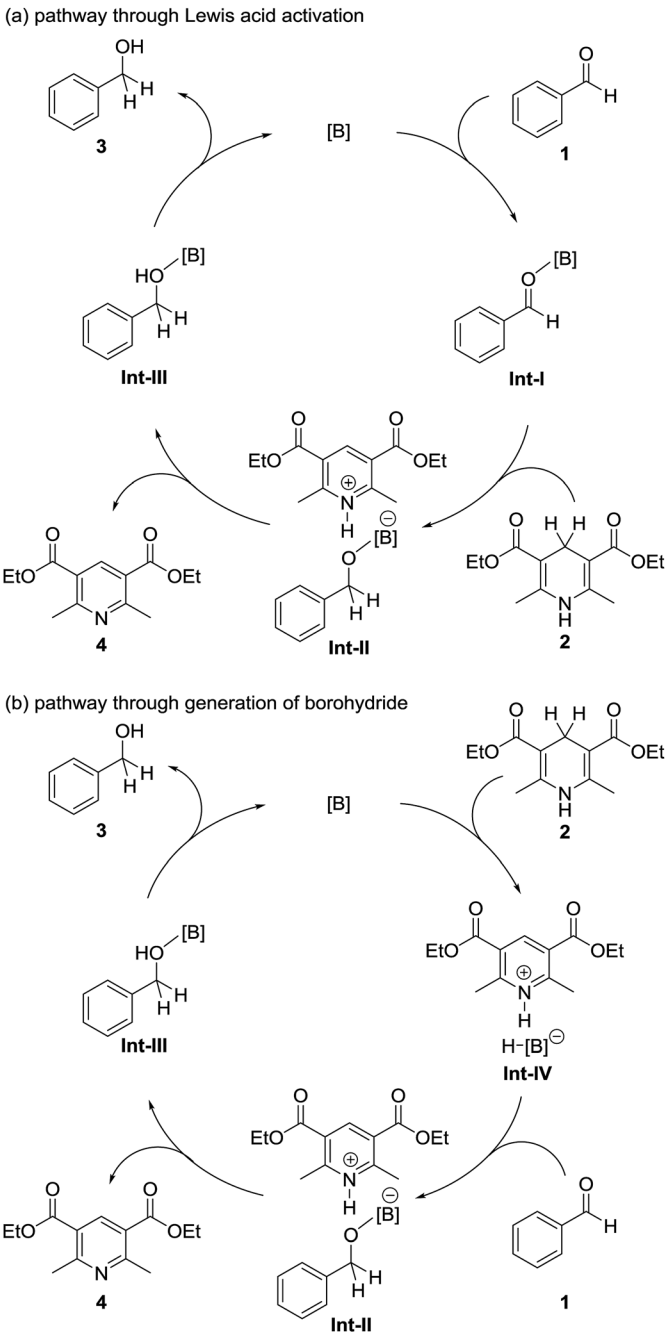

Fig. 2 Possible reaction pathways. (a) Lewis acid activation pathway, (b) borohydride pathway.

Results and discussion

Evaluation of the catalytic activity of borane catalysts in the hydrogenation of benzaldehyde with a Hantzsch ester

To compare the catalytic activity of borane catalysts, we examined the reaction of benzaldehyde (**1**) with the Hantzsch ester **2**

in the presence of a catalytic amount of various borane compounds **B-a** to **B-d** (Scheme 2). When tris[3,5-bis(trifluoromethyl)phenyl]borane (**B-a**) was used as the catalyst, the reaction proceeded efficiently to give benzyl alcohol (**3**) quantitatively. Tris(pentafluorophenyl)borane (**B-b**) also promoted the reaction to give **3** in 88% yield. The catalytic efficiency of **B-a** is therefore superior to that of **B-b**. On the other hand, only a 7% yield of **3** was obtained from the corresponding reaction in the presence of trifluoroborane etherate (**B-c**), whereas triphenylborane (**B-d**) did not promote the reaction at all. These results indicate that the order of catalytic activity is as follows: **B-a** > **B-b** > **B-c** > **B-d**.

Stoichiometric reaction experiments

To identify the reaction pathway, we examined the stoichiometric reactions of **B-a** with benzaldehyde (**1**) and with Hantzsch ester **2** (Scheme 3). In a glove box, **B-a**, **1**, and CD_2Cl_2 were introduced into a J. Young NMR tube (Scheme 3a), and the resulting sample was analyzed by ^{1}H, ^{13}C, and ^{11}B NMR spectroscopy. In the ^{1}H NMR spectrum of this sample, the peak derived from the aldehyde functionality shifted to a higher field (**1**: δ = 10.01 ppm; **Int-Ia**: δ = 9.17 ppm), whereas the peaks derived from the aromatic protons of the benzaldehyde shifted to a lower field (Fig. 3a–c). In the ^{13}C NMR measurement, the peak derived from the aldehyde functionality shifted to a lower field (**1**: δ = 192.6 ppm, **Int-Ia**: δ = 200.2 ppm). These observations suggest that the electron density of the aldehyde functionality decreased after reaction with **B-a**. A high field shift was observed in the ^{11}B NMR measurements (**B-a**: δ = 68.6 ppm, **Int-Ia**: δ = 36.0 ppm), showing that the electron density at the boron center in the resulting product had increased. These results indicated that **Int-Ia** was formed in this reaction. The resulting mixture was also examined by ESI-MS, and a peak corresponding to **Int-Ia** (m/z = 779 $[M + Na]^+$) was observed. The addition of **2** to the reaction mixture then led to further reaction (Scheme 3a). The resulting sample was analyzed by ^{1}H NMR spectroscopy (Fig. 3d). In the ^{1}H NMR spectrum of the resulting mixture, the peak derived from the aldehyde functionality disappeared and a peak derived from benzylic protons appeared (Fig. 3d, inset; δ = 4.53 ppm). **Int-Ia** immediately reacted with **2** to give the benzyl alcohol–tris[3,5-bis(trifluoromethyl)phenyl]borane adduct **Int-IIIa** in 90% NMR yield. GC/MS analysis of the reaction mixture demonstrated the formation of benzyl alcohol (**3**) (m/z = 108 $[M]^+$). In contrast, no peaks arising from the borohydride species **Int-IVa** were observed in the reaction of **B-a** with **2**.[19] If the reaction proceeds *via* a borohydride species (Fig. 2b), **Int-IVa** should have been detected. Therefore, the reaction proceeds through activation of the aldehyde by the boron catalyst, followed by hydride transfer from the Hantzsch ester (Fig. 2a).[20]

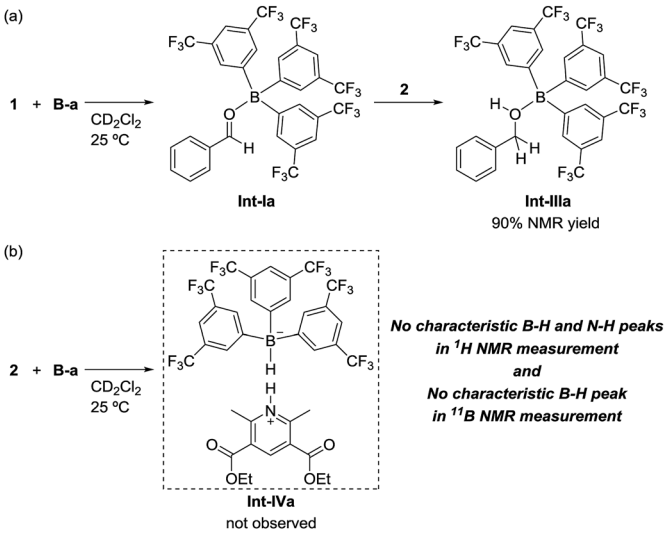

Scheme 3 Stoichiometric experiments on (a) the reaction of benzaldehyde (**1**) with tris[3,5-bis(trifluoromethyl)phenyl]borane (**B-a**) followed by treatment with Hantzsch ester **2**; (b) the reaction of benzaldehyde (**1**) with Hantzsch ester **2**.

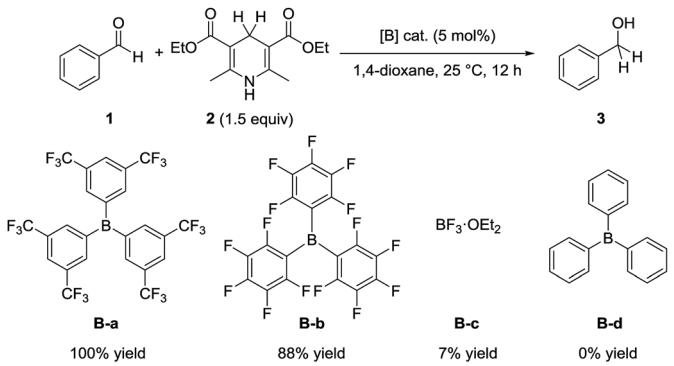

Scheme 2 Hydrogenation of benzaldehyde (**1**) with Hantzsch ester **2**. Reaction conditions: **1** (0.25 mmol), **2** (0.38 mmol), [B] cat. (0.013 mmol), 1,4-dioxane (1 mL), 25 °C, 12 h.

DFT calculations for the hydrogenation of benzaldehyde with a Hantzsch ester catalyzed by various organoboranes

We next performed DFT calculations to elucidate details of our catalytic reaction. All the calculations were carried out with the GAUSSIAN 09 (Revision E.01) program.[21] Geometry optimizations and frequency calculations for all molecules were carried out at the M06-2x[22] level of theory with the basis sets 6-31G(d,p) for C and H and 6-31+G(d,p) for B, N, O, and F. Single-point energies were obtained by calculations at the M06-2x/6-311++G(d,p) level of theory using the SMD[23] solvation model (1,4-dioxane). The energies reported here includes the electronic energy, the zero-point energy, thermal correction at 298.15 K and 1 atm, and solvent-effect correction.

First, we calculated the expected reaction pathway (Scheme 2a). The obtained energy diagram of this catalytic reaction and the calculated structures of transition states are shown in Fig. 4 and 5, respectively. The energy diagram for the reaction with **B-a** is drawn as a red line in Fig. 4. The calculated Gibbs free energy for coordination of **1** to borane **B-a** is −3.7 kcal mol^{-1}, showing that this is an energetically downhill step. The activation energy of the hydride-transfer process is 9.9 kcal mol^{-1}

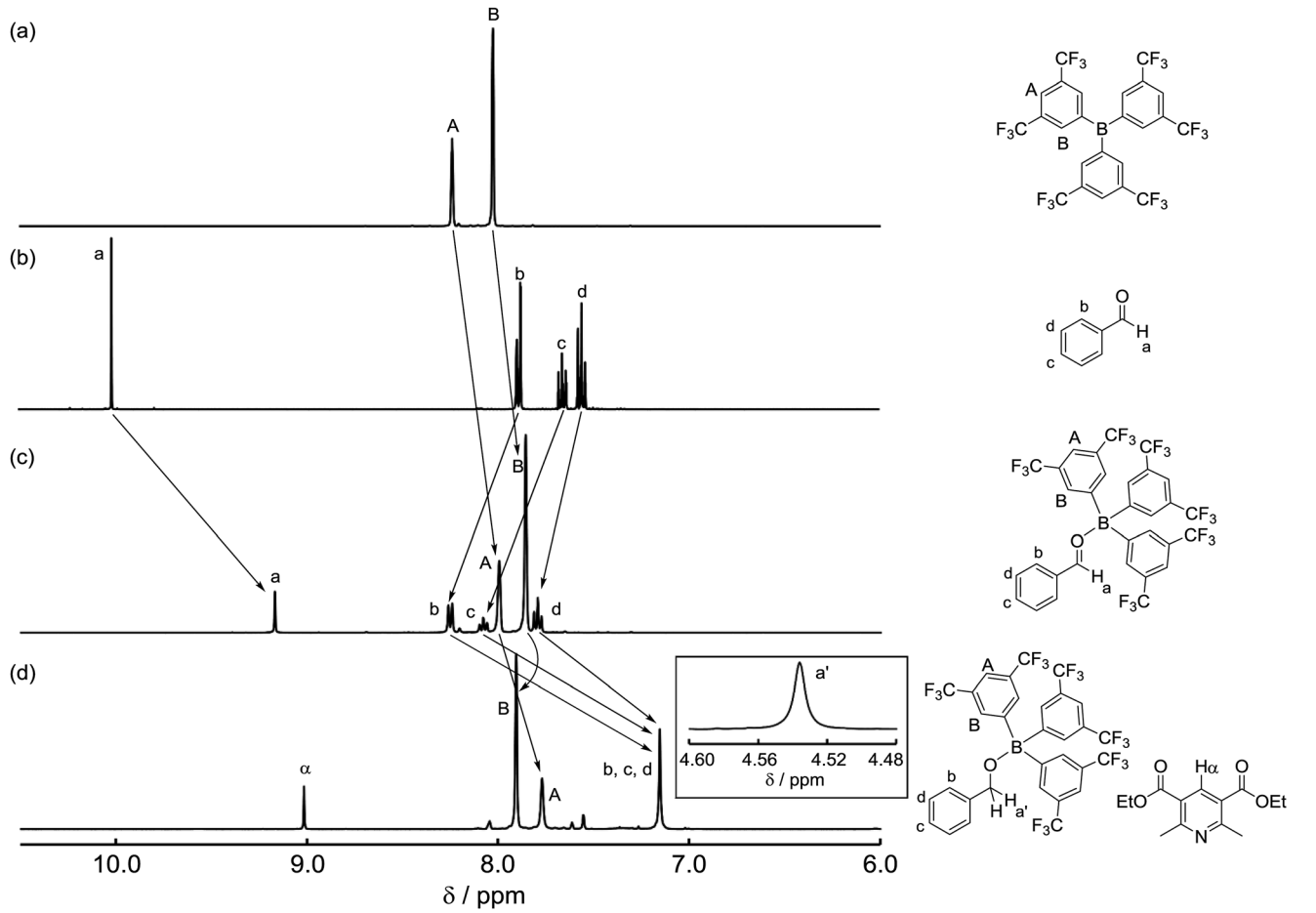

Fig. 3 ^{1}H NMR spectra for (a) tris[3,5-bis(trifluoromethyl)phenyl]borane (**B-a**), (b) benzaldehyde (**1**), (c) a mixture of **1** and **B-a**, and (d) after addition of Hantzsch ester **2** in CD_2Cl_2.

relative to the initial state. The energy difference between **TSa** (Fig. 5a) and [**Int-Ia** + **2**] is 13.6 kcal mol^{-1}. After the hydride transfer, the ionic pair **Int-IIa** is generated and the Gibbs free energy is −8.7 kcal mol^{-1}. Ionic pair **Int-IIa** is more stable than **Int-Ia** ($\Delta\Delta G_{\text{Int-IIa–Int-Ia}} = -5.0$ kcal mol^{-1}). These results show that the hydride-transfer process should proceed smoothly because this step is energetically downhill and has a low activation energy. A proton is then moved to the benzyl alcohol moiety from the protonated Hantzsch pyridine ($\Delta G_{\text{Int-IIIa}} = -9.2$ kcal mol^{-1}, $\Delta\Delta G_{\text{Int-IIIa–Int-IIa}} = -0.5$ kcal mol^{-1}). Finally, **B-a** is liberated from **Int-IIIa** to give **3**. The calculated stabilization energy for the formation of **Int-IIIa** from **B-a** and **3** is −1.1 kcal mol^{-1}. The stabilization energy of the formation of **Int-Ia** is therefore lower than that of the formation of **Int-IIIa**, so the catalytic reaction should proceed smoothly.

We also examined the hydrogenation with **B-b** as the catalyst (Fig. 4; blue line). The formation of **Int-Ib** is a downhill step (stabilization energy −8.9 kcal mol^{-1}). The activation energy of the hydride-transfer process from **2** to **Int-Ib** is 5.3 kcal mol^{-1} relative to the initial state. The energy difference between **TSb** (Fig. 5b) and [**Int-Ib** + **2**] is 14.2 kcal mol^{-1}. This value is slightly greater than the value of the energy difference between **TSa** and [**Int-Ia** + **2**] (13.6 kcal mol^{-1}). After the hydride transfer, **Int-IIb** should be generated ($\Delta G_{\text{Int-IIb}} = -17.2$ kcal mol^{-1}). The ionic intermediate **Int-IIb** is therefore more stable than **Int-Ib** ($\Delta\Delta G_{\text{Int-IIb–Int-Ib}} = -8.3$ kcal mol^{-1}), showing that the reaction should proceed. The Gibbs free energy of **Int-IIIb** is −18.2 kcal mol^{-1}, whereas that for the formation of **Int-IIIb** from **3** and **B-b** is −10.1 kcal mol^{-1}. This value is comparable to the formation of **Int-Ib**: the calculated energy difference is only 1.2 kcal mol^{-1}. These results suggest that the generated **3** suppresses regeneration of the catalyst, thereby explaining why the catalytic activity of **B-b** is lower than that of **B-a**.

The energy diagram for the reaction with **B-c** as the catalyst is shown by the green line in Fig. 4. In this calculations, interaction between diethyl ether and intermediates is not considered. The Gibbs free energy for the formation of **Int-Ic** is 1.9 kcal mol^{-1}. Under the calculation conditions, **B-c** is more stable than **Int-Ic**. However, the energy difference is small. Therefore, formation of **Int-Ic** is possible. For the formation of the ionic-pair intermediate **Int-IIc**, the calculated Gibbs free energy is −8.9 kcal mol^{-1}. The energy difference between **Int-Ic** and **Int-IIc** is therefore −10.8 kcal mol^{-1}, indicating that the hydride-transfer process is energetically downhill. The activation energy for the hydride-transfer process is as high as 16.8 kcal mol^{-1} relative to the initial state, and the energy

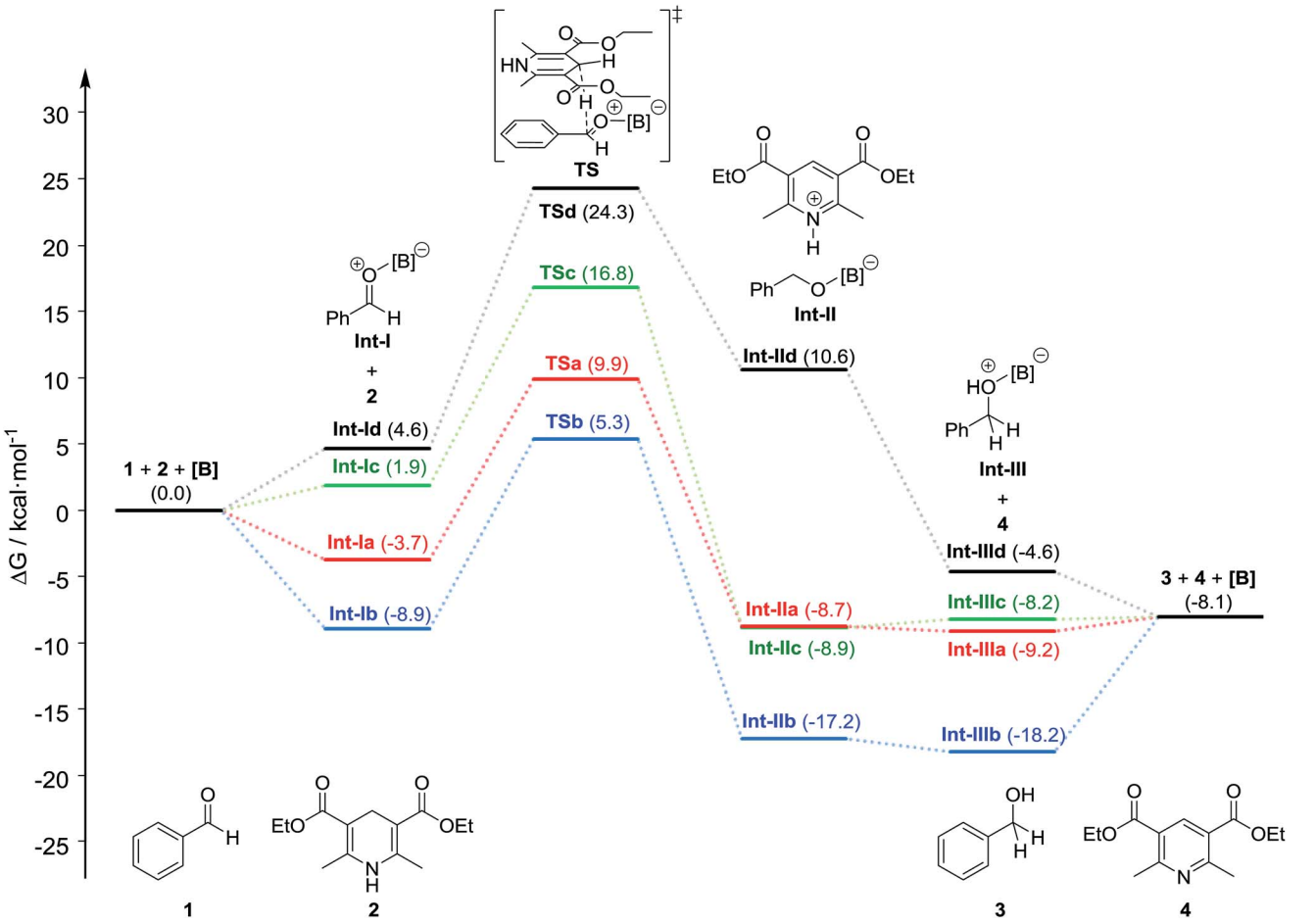

Fig. 4 Energy diagram in the organoborane-catalyzed hydrogenation of benzaldehyde (**1**) with Hantzsch ester (**2**). Red: tris[3,5-bis(trifluoromethyl)phenyl]borane (**B-a**), blue: tris(pentafluorophenyl)borane (**B-b**), green: trifluoroborane etherate (**B-c**), black: triphenylborane (**B-d**).

difference between **TSc** (Fig. 5c) and [**Int-Ic** + **2**] is 14.9 kcal mol^{-1}. These results suggest that the hydride-transfer process should proceed. The activation energy of **TSc** (14.9 kcal mol^{-1}) is larger than that of **TSa** (13.6 kcal mol^{-1}) and **TSb** (14.2 kcal mol^{-1}). The ion-pair intermediate **Int-IIc** should undergo proton transfer to give **Int-IIIc** and **4**, because this process is slightly energetically uphill ($\Delta\Delta G_{\text{Int-IIIc–Int-IIc}}$ = 0.7 kcal mol^{-1}). The formation of **Int-IIIc** from **B-c** and **3** is energetically downhill (−0.1 kcal mol^{-1}). These results suggest that the reaction is difficult due to the higher activation energy barrier and the higher stability of the formation of **Int-IIIc** than that of the formation of **Int-Ic** by 2.0 kcal mol^{-1}. Therefore, when **B-c** was used as the catalyst, **3** was obtained in only 7% yield, because the generated **3** inhibited the formation of **Int-Ic** (Scheme 2).

The energy diagram for the hydrogenation reaction with **B-d** is shown as a black line in Fig. 4. The formation of **Int-Id** is energetically uphill ($\Delta G_{\text{Int-Id}}$ = 4.6 kcal mol^{-1}), suggesting that it is difficult for **1** to coordinate to **B-d**. In the hydride-transfer process, the energy of the desired intermediate **Int-IId** is higher than that of **Int-Id** ($\Delta\Delta G_{\text{Int-IId–Int-Id}}$ = 6.0 kcal mol^{-1}), and the activation energy is relatively high (24.3 kcal mol^{-1} relative to the initial state). Therefore, the hydride-transfer process should not take place. These calculation results suggest that the reaction with **B-d** should not proceed at all.

In our reaction system, the boron catalysts might also react with the Hantzsch ester **2** or with the Hantzsch pyridine **4**. To understand the influence of **2** or **4** on the hydrogenation reaction, we performed DFT calculations for the possible intermediates **Int-IV** to **Int-VIII** (Scheme 4). The results of these calculations are summarized in Table 1. In the case of the reaction of borane **B-a** with **2** and **4**, the Gibbs free energies are 10.9 (**Int-IVa**), 1.0 (**Int-Va**), 18.7 (**Int-VIa**), 7.8 (**Int-VIIa**), and 7.9 kcal mol^{-1} (**Int-VIIIa**), respectively. These reactions should proceed with difficulty, because they are energetically uphill, indicating that **2** and **4** are unlikely to affect the efficiency of the hydrogenation reaction.

On the other hand, in the reaction of **B-b**, the Gibbs free energies for the formation of **Int-IVb** and **Int-Vb** are −4.0 and −2.5 kcal mol^{-1}, respectively. These intermediates might, therefore, be formed in the reaction of **B-b** with **2**. The processes for the formation of **Int-VIb**, **Int-VIIb**, and **Int-VIIIb** are energetically uphill. From these results, the formation of **Int-IIIb** is the most energetically favored of these processes. Therefore, the desired hydrogenation process proceeds and the resulting hydrogenated product **3** partially inhibits the desired formation

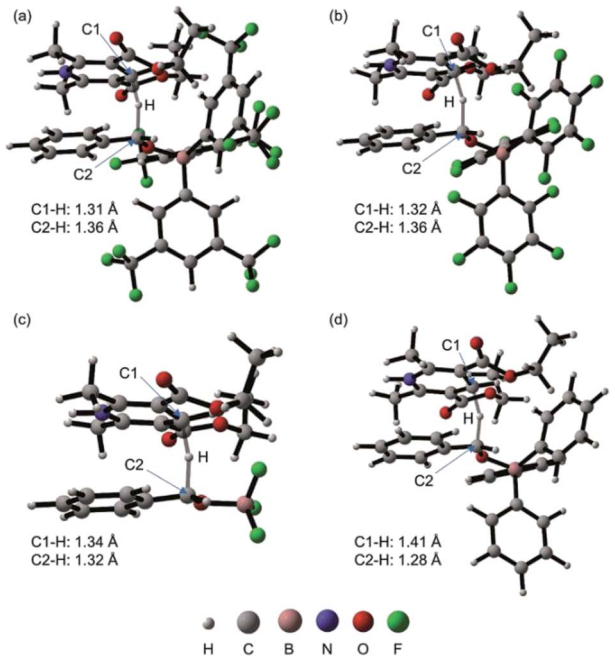

Fig. 5 Calculated structures of transition states TSa (a), TSb (b), TSc (c), and TSd (d) and selected bond distances (the molecular structures were drawn with CYLview[24]).

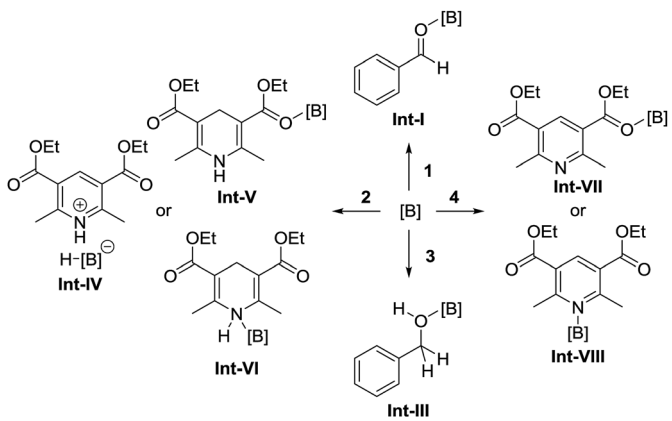

Scheme 4 Possible reactions of boron catalysts in the reaction system.

of **Int-Ib**. The formation of **Int-IVb** and **Int-Vb** might also disturb the formation of **Int-Ib**. Thus, the catalytic activity of **B-b** is lower than that of **B-a**.

In the results of our DFT calculation for the reactions of **B-c** with **2** or **4**, the Gibbs free energies for the formation of **Int-Vc** and **Int-VIIIc** were 1.2 and 1.9 kcal mol^{-1}, respectively. These values are comparable with the Gibbs free energy for the formation of **Int-Ic** (1.9 kcal mol^{-1}). Thus, **2**, **3**, and **4** inhibit the desired reaction, resulting in a low yield of the desired product.

In the reaction of **B-d**, the formation of all intermediates is energetically uphill (by at least 3.5 kcal mol^{-1}). Consequently, the reaction of **B-d** does not proceed at all.

Table 1 Summary of the calculated Gibbs free energies for the expected reactions of boron catalysts (kcal mol^{-1})

	B-a	B-b	B-c	B-d
1	**Int-Ia** (−3.7)	**Int-Ib** (−8.9)	**Int-Ic** (1.9)	**Int-Id** (4.6)
2	**Int-IVa** (10.9)	**Int-IVb** (−4.0)	**Int-IVc** (32.8)	**Int-IVd** (29.9)
	Int-Va (1.0)	**Int-Vb** (−2.5)	**Int-Vc** (1.2)	**Int-Vd** (9.1)
	Int-VIa (18.7)	**Int-VIb** (7.9)	**Int-VIc** (7.0)	**Ind-VId** (−)[a]
3	**Int-IIIa** (−1.1)	**Int-IIIb** (−10.1)	**Int-IIIc** (−0.2)	**Int-IIId** (3.5)
4	**Int-VIIa** (7.8)	**Int-VIIb** (4.6)	**Int-VIIc** (7.0)	**Int-VIId** (16.4)
	Int-VIIIa (7.9)	**Int-VIIIb** (3.4)	**Int-VIIIc** (1.9)	**Int-VIIId** (15.9)

[a] The coordinated structure **Int-VId** was not obtained in the DFT calculation.

Determination of association constants between boron reagents and benzaldehyde or benzyl alcohol

The DFT study indicated that a preferential formation of **Int-I** compared with the formation of **Int-III** is important for the catalytic hydrogenation reaction to proceed. Therefore, we next determined the association constants between boron reagents **B-a** to **B-d** and benzaldehyde (**1**) or benzyl alcohol (**3**). To obtain the association constants, boron compounds **B-a** to **B-d** and **1** or **3** were dissolved in CD_2Cl_2 and subjected to ^{1}H NMR measurements. Variable-temperature (VT) ^{1}H NMR spectra for the reaction of **B-a** with **1** are shown in Fig. 6. The peak derived from the aldehyde functionality separated into peaks derived from uncoordinated benzaldehyde and the coordinated benzaldehyde **Int-Ia** below −40 °C. By using a van't Hoff plot, the association constant was estimated to be 1.19×10^4 M^{-1} (Fig. 7). The Gibbs free energy for the formation of **Int-Ia** was calculated from the association constant to be −5.6 kcal mol^{-1} (Table 2).

We also recorded VT ^{1}H NMR spectra for a mixture of **B-a** and **3** in CD_2Cl_2 (Fig. 8). By using the van't Hoff plot (Fig. 9), the association constant and the Gibbs free energy for the formation of the borane–benzyl alcohol adduct **Int-IIIa** were determined to be 95.4 M^{-1} and –2.7 kcal mol^{-1}, respectively (Table 2). The Gibbs free energy of the formation of **Int-Ia** is lower than that for the formation of **Int-IIIa** ($\Delta\Delta G_{\text{Int-Ia–Int-IIIa}}$ = −2.9 kcal mol^{-1}, Table 2). Therefore, coordination of **B-a** to **1** is preferred to that of **B-a** to **3**, and the desired reaction should proceed smoothly (Scheme 2).

We also measured the VT ^{1}H NMR spectra for the reactions of **B-b** with **1** or **3**.[25] The association constants and the Gibbs free energies for the formation of **Int-Ib** were 396 M^{-1} and –3.5 kcal mol^{-1}, respectively, and those of **Int-IIIb** were 58.3 M^{-1} and –2.4 kcal mol^{-1}, respectively (Table 2).[26] In this case, the difference in the value of the Gibbs free energies for the formation of **Int-Ib** and **Int-IIIb** is −1.1 kcal mol^{-1} (Table 2), so the formation of **Int-Ib** competes with the formation of **Int-IIIb**. Consequently, the catalytic activity of **B-b** should be lower than that of **B-a**.

In the case of $BF_3 \cdot OEt_2$ (**B-c**), the association constant and Gibbs free energy for the formation of **Int-Ic** are 5.51 M^{-1} and –1.0 kcal mol^{-1}, respectively, and the corresponding values for **Int-IIIc** are 263 M^{-1} and –3.3 kcal mol^{-1}, respectively (Table 1).[25]

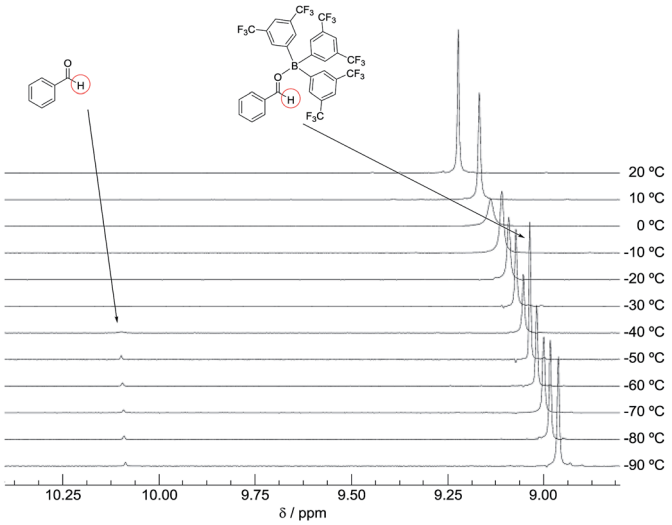

Fig. 6 VT ^{1}H NMR spectra of a mixture of **1** and **B-a** (20 °C to −90 °C).

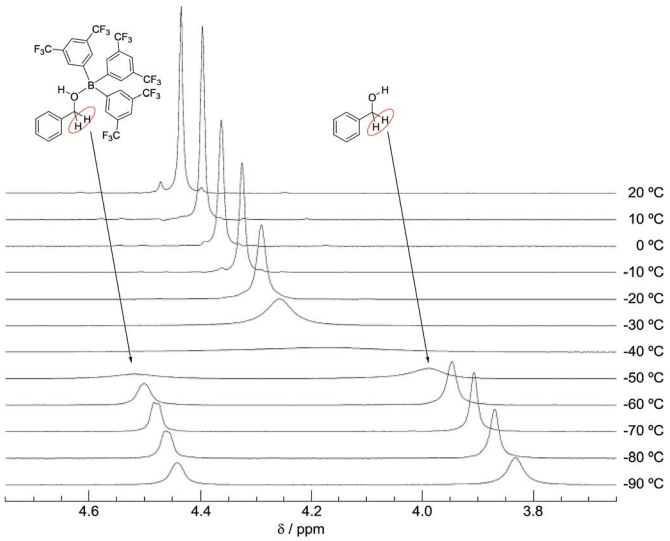

Fig. 8 VT ^{1}H NMR spectra for a mixture of **3** and **B-a** (20 °C to −90 °C).

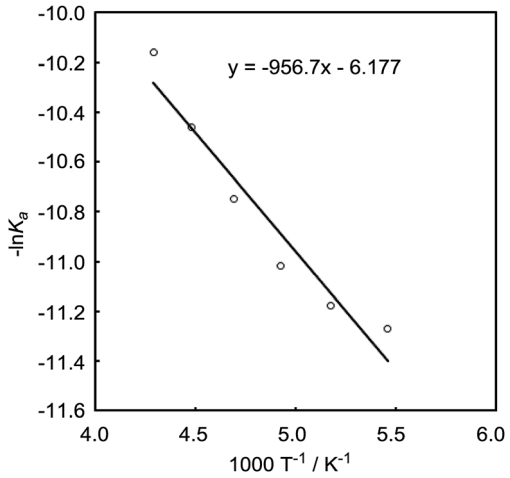

Fig. 7 van't Hoff plot for a mixture of **1** and **B-a** (−40 °C to −90 °C).

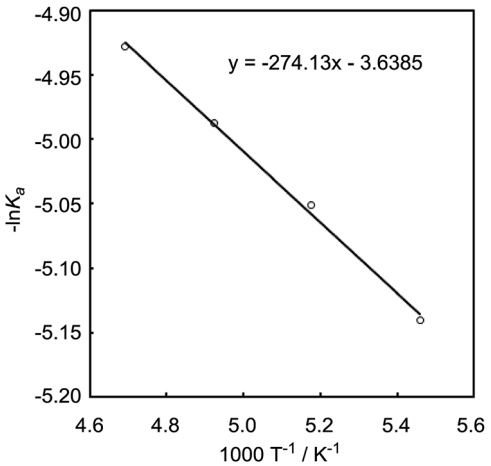

Fig. 9 van't Hoff plot for a mixture of **3** and **B-a** (−60 °C to −90 °C).

The Gibbs free energy for the formation of **Int-IIIc** is therefore lower than that for the formation of **Int-IIIc** ($\Delta\Delta G_{\text{Int-Ic–Int-IIIc}}$ = 2.3 kcal mol^{-1}, Table 2) In the hydrogenation of **1** with **2** with **B-c** as the catalyst, the generated **3** should therefore inhibit the catalytic reaction. Consequently, the reaction does not proceed efficiently (Scheme 2). The order of the catalytic activities of **B-a**, **B-b**, and **B-c** is correlated with the energy differences between the formation of **Int-I** and **Int-III** [catalytic activities: **B-a** > **B-b** > **B-c** (Scheme 2); energy differences between formation of **Int-I** and **Int-III**: **B-a** < **B-b** < **B-c**, (Table 2)].

In the reaction of **B-d** with **1** or **3**, the association constants were 0.195 and 5.67 × 10^{-3} M^{-1}, respectively, and the Gibbs free energies were 1.0 and 3.1 kcal mol^{-1}, respectively (Table 1).[25] These reactions were energetically uphill. Therefore, the

Table 2 Summary of the association constants (K_a) and Gibbs free energy (ΔG) values for the reaction of borane reagents **B-a** to **B-d** with benzaldehyde (**1**) or benzyl alcohol (**3**), as estimated by ^{1}H NMR measurements

	Benzaldehyde (**1**)		Benzyl alcohol (**3**)		
	K_a, M^{-1}	ΔG, kcal mol^{-1}	K_a, M^{-1}	ΔG, kcal mol^{-1}	$\Delta\Delta G_{\text{Int-I–Int-III}}$, kcal mol^{-1}
B-a	1.19 × 10^4	−5.6	95.4	−2.7	−2.9
B-b	396	−3.5	58.3	−2.4	−1.1
B-c	5.51	−1.0	263	−3.3	2.3
B-d	0.195	1.0	5.67 × 10^{-3}	3.1	−2.1

coordination of **1** to **B-d** occurs with difficulty, explaining why the hydrogenation of **1** does not proceed at all in this case (Scheme 2).

Conclusions

We performed NMR experiments and DFT calculations to elucidate the mechanism of the organoborane-catalyzed hydrogenation of benzaldehyde with a Hantzsch ester as a synthetic NADPH analogue, and to explain the activity or lack of activity of various borane catalyst in this reaction. The reactions in the presence of tris[3,5-bis(trifluoromethyl)phenyl] borane, tris(pentafluorophenyl)borane, $BF_3 \cdot OEt_2$, and triphenylborane gave benzyl alcohol in yields of 100, 88, 4, and 0%, respectively. Tris[3,5-bis(trifluoromethyl)phenyl]borane therefore showed a superior catalytic activity to the other borane catalysts in this reaction. Stoichiometric NMR experiments demonstrated that the hydrogenation process proceeds through activation of benzaldehyde by the borane catalyst, followed by hydride transfer from the Hantzsch ester to the activated aldehyde.

DFT calculations for the hydrogenation of benzaldehyde with a Hantzsch ester in the presence of borane catalysts were carried out to elucidate details of the reaction. The activation energies for the hydrogenations in the presence of tris[3,5-bis(trifluoromethyl)phenyl]borane and tris(pentafluorophenyl) borane are sufficiently low to permit the reaction to proceed. However, in the case of tris(pentafluorophenyl)borane, the benzyl alcohol–$B(C_6F_5)_3$ adduct is almost as stable as the benzaldehyde–$B(C_6F_5)_3$ adduct, indicating that the generated benzyl alcohol is likely to inhibit the catalytic cycle. In the case of $BF_3 \cdot OEt_2$, the formation of the BF_3–benzyl alcohol adduct, the BF_3–Hantzsch ester adduct, and the BF_3–Hantzsch pyridine adduct should retard the formation of the BF_3–benzaldehyde adduct, explaining why the catalytic reaction does not proceed efficiently. In contrast, the activation energy in the reaction with triphenylborane is relatively high and the hydrogen-transfer process is energetically uphill, explaining why the reaction proceeds with difficulty. These results explain why tris[3,5-bis(trifluoromethyl)phenyl]borane is superior to the other boron catalysts in this hydrogenation reaction.

Association constants and Gibbs free energies for the reaction of boron catalysts with benzaldehyde and benzyl alcohol were determined by ^{1}H NMR analyses. In the case of tris[3,5-bis(trifluoromethyl)phenyl]borane, the association constant of formation of the borane–benzaldehyde adduct is greater than that for the formation of the borane–benzyl alcohol adduct, explaining why the desired catalytic hydrogenation proceeds smoothly. The association constant of tris(pentafluorophenyl) borane with benzaldehyde is comparable to that of tris(pentafluorophenyl)borane with benzyl alcohol, indicating that the formation of the benzaldehyde–$B(C_6F_5)_3$ adduct competes with the formation of the benzyl alcohol–$B(C_6F_5)_3$ adduct. Consequently, the catalytic activity of tris(pentafluorophenyl)borane is lower than that of tris[3,5-bis(trifluoromethyl)phenyl]borane. On the other hand, in the reaction of $BF_3 \cdot OEt_2$, the association constant for the formation of the benzaldehyde–BF_3 adduct is lower than that for the BF_3–benzyl alcohol adduct. The generation of benzyl alcohol therefore inhibits the hydrogenation of benzaldehyde when $BF_3 \cdot OEt_2$ is used as a catalyst. The association constants of triphenylborane with benzaldehyde and benzyl alcohol are low, suggesting the hydrogenation reaction should not proceed efficiently. These experimental results also demonstrated why tris[3,5-bis(trifluoromethyl)phenyl]borane is a superior catalyst to the other borane catalysts in the hydrogenation reaction.

Conflicts of interest

There are no conflicts to declare.

Acknowledgements

This research project was supported by JST-ACCEL program (JPMJAC1401). G. H. appreciates funding from the JSPS-KAKENHI [Grant-in-Aid for Young Scientists (B) No. 17K14524]. The calculations were performed at the Research Center for Computational Science, Okazaki, Japan.

Notes and references

1 J. M. Berg, J. L. Tymoczko and L. Stryer, *Biochemistry*, W. H. Freeman, New York, 5th edn, 2001.

2 For selected recent reviews on enzymatic reduction of carbonyl compounds, see; (*a*) M. Kataoka, K. Kita, M. Wada, Y. Yasohara, J. Hasegawa and S. Shimizu, *Appl. Microbiol. Biotechnol.*, 2003, **62**, 437; (*b*) L. R. Jarboe, *Appl. Microbiol. Biotechnol.*, 2011, **89**, 249; (*c*) C. A. Rabinovitch-Deere, J. W. K. Oliver, G. M. Rodriguez and S. Atsumi, *Chem. Rev.*, 2013, **113**, 4611.

3 For selected recent reviews on transfer hydrogenation using synthetic NADH analogues as the hydrogen donors, see; (*a*) S.-L. You, *Chem.–Asian J.*, 2007, **2**, 820; (*b*) S. G. Ouellet, A. M. Walji and D. W. C. Macmillan, *Acc. Chem. Res.*, 2007, **40**, 1327; (*c*) M. Rueping, E. Sugiono and F. R. Schoepke, *Synlett*, 2010, **21**, 852; (*d*) M. Rueping, J. Dufour and F. R. Schoepke, *Green Chem.*, 2011, **13**, 1084; (*e*) J. G. de Vries and N. Mršić, *Catal. Sci. Technol.*, 2011, **1**, 727; (*f*) C. Zheng and S.-L. You, *Chem. Soc. Rev.*, 2012, **41**, 2498; (*g*) A. M. F. Philips and A. J. L. Pomberio, *Org. Biomol. Chem.*, 2017, **15**, 2307.

4 A. McSkimming and S. B. Colbran, *Chem. Soc. Rev.*, 2013, **42**, 5439.

5 For catalytic transfer hydrogenation of imines with a Hantzsch ester, see; (*a*) M. Rueping, C. Azap, E. Sugiono and T. Theissmann, *Synlett*, 2005, 2367; (*b*) M. Rueping, E. Sugiono, C. Azap, T. Theissmann and M. Bolte, *Org. Lett.*, 2005, **7**, 3781; (*c*) S. Hoffmann, A. M. Seayad and B. List, *Angew. Chem., Int. Ed.*, 2005, **44**, 7424; (*d*) T. B. Nguyen, H. Bousserouel, Q. Wang and F. Guéritte, *Adv. Synth. Catal.*, 2011, **353**, 257; (*e*) T. B. Nguyen, Q. Wang and F. Guéritte, *Chem.–Eur. J.*, 2011, **17**, 9576; (*f*) P. Bachu, C. Zhu and T. Akiyama, *Tetrahedron Lett.*, 2013, **54**, 3977; (*g*) T. Akiyama, K. Saito, S. Janczak and

Z. J. Lesnikowsiki, *Synlett*, 2014, **25**, 795; (*h*) V. N. Wakchaure, P. S. J. Kaib, M. Leutzsch and B. List, *Angew. Chem., Int. Ed.*, 2015, **54**, 11852; (*i*) J. Chen, Z. Zhang, Z. Bao, Y. Su, H. Xing, Q. Yang and Q. Ren, *ACS Appl. Mater. Interfaces*, 2017, **9**, 9772; (*j*) Q. Wang, J. Chen, X. Feng and H. Du, *Org. Biomol. Chem.*, 2018, **16**, 1448.

6 For catalytic transfer hydrogenation of α,β-unsaturated carbonyls with a Hantzsch ester, see; (*a*) J. W. Yang, M. T. Hechavarria Fonseca and B. List, *Angew. Chem., Int. Ed.*, 2004, **43**, 6660; (*b*) J. W. Yang, M. T. Hechavarria Fonseca, N. Vignola and B. List, *Angew. Chem., Int. Ed.*, 2005, **44**, 108; (*c*) S. G. Ouellet, J. B. Tuttle and D. W. C. MacMillan, *J. Am. Chem. Soc.*, 2005, **127**, 32; (*d*) S. Mayer and B. List, *Angew. Chem., Int. Ed.*, 2006, **45**, 4193; (*e*) J. B. Tuttle, S. G. Ouellet and D. W. C. MacMillan, *J. Am. Chem. Soc.*, 2006, **128**, 12662; (*f*) N. J. A. Martin and B. List, *J. Am. Chem. Soc.*, 2006, **128**, 13368; (*g*) G.-L. Zhao and A. Córdova, *Tetrahedron Lett.*, 2006, **47**, 7417; (*h*) T. J. Hoffman, J. Dash, J. H. Rigby, S. Arseniyadis and J. Cossy, *Org. Lett.*, 2009, **11**, 2756; (*i*) K. Akagawa, H. Akabane, S. Sakamoto and K. Kudo, *Tetrahedron: Asymmetry*, 2009, **20**, 461; (*j*) J. Che and Y. Lam, *Synlett*, 2010, 2415; (*k*) C. Ebner and A. Pfaltz, *Tetrahedron*, 2011, **67**, 10287; (*l*) D. B. Ramachary, R. Sakthidevi and P. S. Reddy, *RSC Adv.*, 2013, **3**, 13497.

7 For catalytic transfer hydrogenations of α-keto esters with a Hantzsch ester, see; J. W. Yang and B. List, *Org. Lett.*, 2006, **8**, 5653.

8 For Brønsted acid-mediated transfer hydrogenation of nonactivated aldehydes with synthetic NADH analogues, see; (*a*) S. Shinkai, H. Hamada and O. Manabe, *Tetrahedron Lett.*, 1979, **20**, 1397; (*b*) S. Fukuzumi, M. Ishikawa and T. Tanaka, *J. Chem. Soc., Chem. Commun.*, 1985, 1069; (*c*) S. Fukuzumi, M. Ishikawa and T. Tanaka, *Tetrahedron*, 1986, **42**, 1021; (*d*) M. Ishikawa and S. Fukuzumi, *J. Chem. Soc., Chem. Commun.*, 1990, 1353; (*e*) K. Kuroda, T. Nagamatsu, R. Yanada and F. Yoneda, *J. Chem. Soc., Perkin Trans. 1*, 1993, 547.

9 For Lewis acid-mediated hydrogenation of nonactivated aldehydes with synthetic NADH analogues, see; (*a*) D. J. Creighton and D. S. Sigman, *J. Am. Chem. Soc.*, 1971, **93**, 6314 (Zn); (*b*) M. Shirai, T. Chishina and M. Tanaka, *Bull. Chem. Soc. Jpn.*, 1975, **48**, 1079 (Zn, Pb, Cb, Cu); (*c*) D. J. Creighton, J. Hajdu and D. S. Sigman, *J. Am. Chem. Soc.*, 1976, **98**, 4619 (Zn). (*d*) Y. Ohnishi and M. Kitami, *Tetrahedron Lett.*, 1978, **19**, 4033 (Mg); (*e*) M. Hughes and R. H. Prince, *J. Inorg. Nucl. Chem.*, 1978, **40**, 703 (Zn, Ni); (*f*) R. A. Hood and R. H. Prince, *J. Chem. Soc., Chem. Commun.*, 1979, 163 (Zn); (*g*) R. Mathis, G. Dupas, A. Decormeille and G. Quéguiner, *Tetrahedron Lett.*, 1981, **22**, 59 (Mg); (*h*) A. Ohno, Y. Ishihara, S. Ushida and S. Oka, *Tetrahedron Lett.*, 1982, **23**, 3185 (B, Ti, Al, Zr, Sb); (*i*) G. Dupas, J. Bourguignon, C. Ruffin and G. Quéguiner, *Tetrahedron Lett.*, 1982, **23**, 5141 (Mg); (*j*) H. Awano and W. Tagaki, *J. Chem. Soc., Chem. Commun.*, 1985, 994 (Zn). (*k*) J. Cazin, G. Dupas, J. Bourguignon and G. Quéguiner, *Tetrahedron Lett.*, 1986, **27**, 2375 (Mg); (*l*) J. F. J. Engbersen, A. Koudijs and H. C. van der Plas, *Bioorg. Chem.*, 1988, **16**, 215 (Zn); (*m*) G. Gelbard, J. Lin and N. Roques, *J. Org. Chem.*, 1992, **57**, 1789 (Mg, Zn, Nd, La, Eu, Al).

10 G. Hamasaka, H. Tsuji and Y. Uozumi, *Synlett*, 2015, **26**, 2037.

11 (*a*) L. Deloux and M. Srebnik, *Chem. Rev.*, 1993, **93**, 763; (*b*) P. J. Duggan and E. D. Tyndall, *J. Chem. Soc., Perkin Trans. 1*, 2002, 1325; (*c*) K. Ishihara, in *Boronic Acids: Preparation and Applications in Organic Synthesis and Medicine*, ed. D. G. Hall, Wiley-VCH, Weinheim, ch. 10, 2005, pp. 377–409; (*d*) E. Dimitrijević and M. S. Taylor, *ACS Catal.*, 2013, **3**, 945.

12 (*a*) W. E. Piers and T. Chivers, *Chem. Soc. Rev.*, 1997, **26**, 345; (*b*) K. Ishihara and H. Yamamoto, *Eur. J. Org. Chem.*, 1999, 527; (*c*) G. Erker, *Dalton Trans.*, 2005, 1883; (*d*) W. E. Piers, *Adv. Organomet. Chem.*, 2005, **52**, 1.

13 (*a*) D. W. Stephan and G. Erker, *Angew. Chem., Int. Ed.*, 2010, **49**, 46; (*b*) D. W. Stephan and G. Erker, *Top. Curr. Chem.*, 2013, **332**, 85; (*c*) J. Paradies, *Synlett*, 2013, **24**, 777; (*d*) J. Paradies, *Angew. Chem., Int. Ed.*, 2014, **53**, 3552; (*e*) D. W. Stephan, *Acc. Chem. Res.*, 2015, **48**, 306; (*f*) M. Oestreich, J. Hermeke and J. Mohr, *Chem. Soc. Rev.*, 2015, **44**, 2202; (*g*) D. W. Stephan, *Science*, 2016, **354**, aaf7229; (*h*) W. Meng, X. Feng and H. Du, *Acc. Chem. Res.*, 2018, **51**, 191.

14 Combinations of $B(C_6F_5)_3$ and an ether (Et_2O, i-Pr_2O, or 1,4-dioxane) catalyze the hydrogenation of ketones and some aldehydes with H_2 gas, see: (*a*) T. Mahdi and D. W. Stephan, *J. Am. Chem. Soc.*, 2014, **136**, 15809; (*b*) D. J. Scott, M. J. Fuchter and A. E. Ashley, *J. Am. Chem. Soc.*, 2014, **136**, 15813.

15 A combination of $B(C_6F_5)_3$ and cyclodextrin or molecular sieves also catalyzed the hydrogenation of ketones and aldehydes with H_2 gas; see: T. Mahdi and D. W. Stephan, *Angew. Chem., Int. Ed.*, 2015, **54**, 8511.

16 J. D. Webb, V. S. Laberge, S. J. Geier, D. W. Stephan and C. M. Crudden, *Chem.–Eur. J.*, 2010, **16**, 4895.

17 I. Chatterjee and M. Oestreich, *Angew. Chem., Int. Ed.*, 2015, **43**, 1965.

18 S. Keess and M. Oestreich, *Chem. Sci.*, 2017, **8**, 4688.

19 See Fig. S1 in ESI.†

20 Very recently, Melen, Oestreich, and co-workers reported a tris[3,5-bis(trifluoromethyl)phenyl]borane-catalyzed hydroboration of imines. They also proposed a similar Lewis acid activation pathway; see; Q. Yin, Y. Soltani, R. L. Melen and M. Oestreich, *Organometallics*, 2017, **36**, 2381.

21 M. J. Frisch, G. W. Trucks, H. B. Schlegel, G. E. Scuseria, M. A. Robb, J. R. Cheeseman, G. Scalmani, V. Barone, B. Mennucci, G. A. Petersson, H. Nakatsuji, M. Caricato, X. Li, H. P. Hratchian, A. F. Izmaylov, J. Bloino, G. Zheng, J. L. Sonnenberg, M. Hada, M. Ehara, K. Toyota, R. Fukuda, J. Hasegawa, M. Ishida, T. Nakajima, Y. Honda, O. Kitao, H. Nakai, T. Vreven, J. A. Montgomery Jr, J. E. Peralta, F. Ogliaro, M. Bearpark, J. J. Heyd, E. Brothers, K. N. Kudin, V. N. Staroverov, T. Keith, R. Kobayashi, J. Normand, K. Raghavachari, A. Rendell, J. C. Burant, S. S. Iyengar, J. Tomasi, M. Cossi, N. Rega,

J. M. Millam, M. Klene, J. E. Knox, J. B. Cross, V. Bakken, C. Adamo, J. Jaramillo, R. Gomperts, R. E. Stratmann, O. Yazyev, A. J. Austin, R. Cammi, C. Pomelli, J. W. Ochterski, R. L. Martin, K. Morokuma, V. G. Zakrzewski, G. A. Voth, P. Salvador, J. J. Dannenberg, S. Dapprich, A. D. Daniels, O. Farkas, J. B. Foresman, J. V. Ortiz, J. Cioslowski and D. J. Fox, *GAUSSIAN 09 (Revision E.O1)*, Gaussian, Inc., Wallingford, 2013.

22 Y. Zhao and D. G. Truhalar, *Theor. Chem. Acc.*, 2008, **120**, 215.

23 A. V. Marenich, C. J. Cramer and D. G. Truhlar, *J. Phys. Chem. B*, 2009, **113**, 6378.

24 C. Y. Legault, *CYLview, 1.0b*, Université de Sherbrooke, Canada, 2009, http://www.cylview.org.

25 See ESI.†

26 Piers and co-workers determined the association constant for the formation of **Int-Ib** [$K_a = 2.1(1) \times 10^4$] by another ^{1}H NMR technique (not VT ^{1}H NMR) in C_6D_6: see; D. J. Parks, W. E. Piers, M. Parvez, R. Atencio and M. J. Zaworotko, *Organometallics*, 1998, **17**, 1369. In our study, the association constant was obtained by VT ^{1}H NMR measurements on a 1 : 1 (molar) mixture of **B-b** and **1** in CD_2Cl_2. Because the solubility of **B-a** for C_6D_6 is low, we chose CD_2Cl_2 as the solvent for our NMR experiments. The different solvent and measurement method might have affected the result.